

MSc Project - Binding Affinity Prediction of Protein-Ligand Complex

Abdus Salam Khazi
abdus.khazi@students.uni-freiburg.de

[Github Repository](#) [6]

Supervisors: Simon Bray & Alireza Khanteymoori

September 26, 2021

Contents

| | | |
|----------|--|----------|
| 1 | Abstract | 3 |
| 2 | Introduction | 4 |
| 2.1 | Biological Background | 4 |
| 2.2 | Understanding Binding Affinity | 5 |
| 2.3 | PDBBind Dataset | 5 |
| 3 | Methods | 6 |
| 3.1 | Problem Formulation | 6 |
| 3.1.1 | Problem Overview | 6 |
| 3.1.2 | File formats overview | 7 |
| 3.2 | Extraction of features | 9 |
| 3.2.1 | Ligand Features using RDKit | 9 |
| 3.2.2 | Protein Features using fpocket/dpocket descriptors | 9 |
| 3.3 | Feature selection | 10 |
| 3.3.1 | Requirement of feature selection | 10 |
| 3.3.2 | Feature Family analysis | 10 |
| 3.3.3 | Feature Selection Strategies | 11 |
| 3.4 | Testing | 13 |
| 3.4.1 | Reproducibility | 13 |
| 3.4.2 | Model Quality Analysis | 13 |

| | | |
|----------|--|-----------|
| 4 | Results | 14 |
| 4.1 | Data Preprocessing | 15 |
| 4.1.1 | Data cleaning | 15 |
| 4.1.2 | Dealing with measurement resolution | 16 |
| 4.2 | Linear regression | 18 |
| 4.2.1 | Score function of genetic feature selection | 19 |
| 4.2.2 | Initialization strategies of population | 20 |
| 4.3 | Random Forest Regression | 21 |
| 4.3.1 | Dealing with correlated features | 22 |
| 4.3.2 | Dealing with measurement resolution | 23 |
| 4.3.3 | Feature Importance calculation | 24 |
| 4.3.4 | Permutation Importance and genetic algorithm | 24 |
| 4.4 | Support Vector Regression | 25 |
| 4.5 | Rotation Forests | 26 |
| 5 | Discussion | 28 |
| 6 | Conclusion | 30 |
| 7 | Appendix | 32 |
| 7.1 | XYZ File format | 32 |
| 7.2 | SDF File format | 32 |
| 7.3 | MOL2 File Format | 33 |
| 7.4 | Correlation Heat Maps | 34 |

1 Abstract

2 Introduction

2.1 Biological Background

Proteins are the workhorses of our body. They are necessary for many essential functions in the body. Ligands are molecules that bind to proteins to form protein-ligand complexes. They can be molecules that the protein transports (e.g., a Haemoglobin transporter). They can also act as stimulating agents. In addition to this, the ligands can also start/stop the protein from doing its function. The correct functioning of these protein-ligand complexes is thus essential for any living organism.

The study of protein-ligand complexes is an intrinsic part of the drug discovery field. It is because drugs are small molecules that act as ligands. As the drug molecules (ligands) bind to the target proteins, they can artificially influence the protein behavior. This binding between protein and ligand causes a therapeutic effect.



Figure 1: Haemoglobin transporter protein. [15]

When one finds a target drug candidate, one has to answer questions like - How easily does the drug bind to the target protein? Does it bind to any other protein - If so, is it desirable? Does it have any unforeseen effect on the protein function? To answer these questions, biologists and pharmacists conduct wet-lab experiments that are expensive.

One way to reduce the cost of these experiments is to make a data-driven selection of the drugs. Using experimental data collected over many

years, one can build models to predict the behavior of the proposed drug computationally. These 'In-Silico' computational methods can aid in the elimination of undesirable drug candidates as well as guide the drug selection process.

This project aims to answer one of the above questions - How well does a given drug bind to the target protein? It is determined computationally by building a machine learning model that trains on data collected over the past decades. The goal of the project is to reduce drug discovery costs using the ML model.

2.2 Understanding Binding Affinity

Binding affinity between a protein and a ligand is quantified by the K_d , K_i and IC_{50} measures in the PDBind Data bank. Here K_d refers to the dissociation constant, K_i to inhibition constant, and IC_{50} to inhibitory concentration 50%. The reason for having different measurements is because it is not possible to use the same measurement techniques for all biological complexes/processes.

To understand K_d , consider a protein and a ligand binding and unbinding continuously in a kinetic system. In this system, let $[P]$, $[L]$, and $[PL]$ represent the concentrations of the Protein, the Ligand, and the Protein-Ligand complex. This is represented by the following equation:



The binding affinity K_d can be quantified by using the concentrations in the above system at equilibrium.

$$K_d = \frac{[P][L]}{[PL]} = \frac{k_{-1}}{k_1}$$

where k_{-1} is the dissociation rate constant and k_1 is the association rate constant. Similarly, K_i and IC_{50} are defined using concentration albeit non-trivially. [11]

2.3 PDBind Dataset

Over the last few decades, researchers have been successful in building a single data archive for proteins. This archive, called **Protein Data Bank** [8], holds 3-D structural data of the proteins determined by experiments like X-ray crystallographic, Nuclear magnetic resonance (NMR), and cryoelectron microscopy (cryoEM). A subset of this data also contains information about

the binding affinity between a protein and ligands. Moreover, it contains information on protein-protein complexes. [7]

This project aims to study the protein-ligand binding affinity. Hence, only the binding affinity data between the proteins and the ligands should be extracted from **Protein Data Bank**. A dataset called **PDBBind Data Bank** already does this [13]. Using the curated protein-ligand affinity data present in the PDBBind Data bank, the project builds a machine learning model that learns to predict this affinity.

3 Methods

3.1 Problem Formulation

3.1.1 Problem Overview

The problem that is solved is - *Given $K_d/K_i/IC_{50}$ for various complexes in the PDBBind Data bank, can this affinity measure be predicted for new protein-ligand complexes?* Figure 2 shows how the Protein-Ligand problem can be classified.

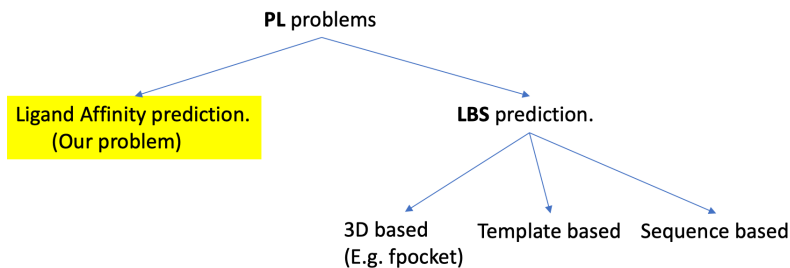


Figure 2: Protein-Ligand problem classification.

The 3D structure of proteins and ligands strongly influences how they bind. Figure 3 illustrates a hypothesis called *Lock and Key*. The shape of the protein’s binding location and the shape of the ligand must be complementary for the binding.

Any potential binding location in the 3D structure of a protein is called a pocket. The other parts of the protein do not have a direct influence during the binding. Hence only pocket features are extracted from the data. A 3D-based LBS prediction package called *fpocket* is used to find the potential pockets. A submodule in the package, called *dpocket*, is used to extract the binding pocket’s features.



Figure 3: Lock and Key hypothesis in molecular docking. [12]

The features of proteins and ligands are kept separate till the training phase as much as possible. In other words, the features are not concatenated before the preprocessing of the ML pipeline (For example, before the output correlation calculation). It helps the model's input become plug and play. Hence, the binding affinity between any protein and any ligand is predictable by the trained model. However, one must note that the concatenation of features is done during the feature selection phase using genetic algorithms because the training of models is a requirement for running them (Section 3.3.3).

3.1.2 File formats overview

The **PDBBind Data bank** extracts information about the PL complexes from the **Protein Data bank** and creates the following files for every complex

- **PDB Format** - For the Protein.
- **Mol2** - For the ligand.
- **SDF** - For the ligand.

All of the above formats contain the essential 3D structural information required for predicting the binding affinity. These formats use the **XYZ format** internally to represent the 3D structure of their molecules.

XYZ format: XYZ format is a chemical file format that represents the geometry of a molecule. It specifies the atoms in a molecule along with their cartesian coordinates in the X, Y, and Z-axes. Hence it is named *XYZ format*. The following text illustrates the format. Section 7.1 gives a detailed example. [18]

```
<number of atoms>
comment line
<element> <X> <Y> <Z>
...
```

The unit of distance used in this format is Angstrom (\AA). $1 \text{\AA} = 10^{-10}$ m. [18]

PDB format: PDB format is a human-readable file format used to represent the protein molecules (macromolecules). Within the PDB format, the coordinates of atoms are represented like the XYZ format. Because of the 3D information in this format, molecular visualization of proteins is possible with specialized software. It also contains information about atomic connectivity and the protein’s primary, secondary, tertiary, and quaternary structures. [14] [4] Please see [1] for an example pdb file.

Structure Data File (SDF) Format: SDF format file is a Chemical Table file (CT File) that contains a structure of the molecule in the XYZ format. It contains information like atomic bonds, connectivity information, molecular weight, and molecular formula. [17] Section 7.2 illustrates the SDF file format.

Mol2 format: Similar to the SDF format, Mol2 also represents the 3D structure of molecules in the XYZ format. It contains the atomic bond and connectivity information but does not contain the other data like molecular weight and formula. The ligands given in this format are used in the project because features of more ligands could be extracted using the RDKit feature extractor. Section 7.3 illustrates the Mol2 file format in more detail.

SMILES format: SMILES is an acronym for Simplified Molecular-Input Line-Entry System. It represents a molecule using an ASCII string. Using the 3D data in SDF and Mol2 formats, a graph representing the 3D molecular structure can be created (where nodes are atoms and edges are atomic bonds). Using graph traversal algorithms, the SMILES string for the

molecule can be generated. The SMILES format itself is not very helpful for us as one would lose the 3D structural information after converting to it. Nevertheless, it is a useful format to represent the molecules compactly. [16]

3.2 Extraction of features

As the file formats are different for proteins and ligands, different tools were used to extract their features.

3.2.1 Ligand Features using RDKit

RDKit is an open-source cheminformatics software library [9]. The core data structures and algorithms of RDKit are written in C++, and the Python wrappers are generated using the *Boost.Python* package. Using the module *RDKit.Chem.Descriptors*, 402 features were extracted for each ligand [2]. Each descriptor value is encoded as a real-valued number, hence the ligand feature space is \mathbf{R}^{402} before any feature elimination.

3.2.2 Protein Features using fpocket/dpocket descriptors

Fpocket stands for "Find pocket" whereas *Dpocket* stands for "Describe pocket". *Fpocket* uses 3D Voronoi tessellation and the concepts of "Alpha Spheres" to find out pockets in the protein structure [5] [19]. The descriptors (features) of all pockets in the protein are extracted from the given protein PDB file. For every pocket, 55 descriptors are obtained in total. They are taken as real-valued numbers, \mathbf{R} . Hence, the input space for protein features is \mathbf{R}^{55} .

The descriptors of the ligand-binding pockets are extracted from *Dpocket*. *Dpocket* is provided with the protein PDB file and the ligand ID of the PL complex as input. It generates three files as output files, namely, *dpout_fpocketp.txt*, *dpout_fpocketnp.txt*, and *dpout_explicitp.txt*.

- **dpout_fpocketp.txt.** This file contains the descriptors (a.k.a features) of all the pockets that are the binding pockets based on a criterion. The ligand can bind at different locations (pockets) in the protein 3D structure. Hence, there may be features of more than one pocket in this file.
- **dpout_fpocketnp.txt.** This file contains the descriptors of all pockets that are non-binding according to the criterion.

- **dpout_explicitp.txt**. This file contains the descriptors of all explicit pockets in the PL complex. An explicit pocket is a pocket that consists of all vertices/atoms situated at a specific distance from the ligand in the PL complex. This distance is 4 Å by default.

In the project, dpout_fpocketnp.txt files are not used as they contain the non-binding pockets. The pocket descriptors of the dpout_fpocketp.txt file are preferred because explicitly defined pockets of **dpout_explicitp.txt** are heavily biased towards the ligand.

3.3 Feature selection

3.3.1 Requirement of feature selection

Both the protein and the ligand are equally responsible for the affinity of the PL complex. Hence their descriptors were concatenated to get a high dimensional \mathbf{R}^{457} input for the model. There are a couple of issues with using all of the descriptors.

- The amount of data is not very large. For example, only ≈ 35000 data points could be obtained after concatenating the ligand features with the *fpocketp* pocket descriptors.
- The number of ligand descriptors \gg protein descriptors. It creates a data imbalance and may lead the model to select only ligand features for their prediction.

Hence some methods to reduce the input dimensions are required.

3.3.2 Feature Family analysis

The features extracted from the PDB files and the ligand files can be classified into various families. Some of the important ones are - AUTOCORR2d_, Chi, EState_VSA, PEOE_VSA, SMR_VSA, SlogP_VSA, VSA_EState, and fr_. Figure 4 shows the correlation matrices of 2 families, AUTOCORR2d_ and Chi. As can be seen in the heatmap, there is a heavy correlation between features within these families. Hence a strategy to deal with this is also required. The correlation heat maps for the other families are shown in section 7.4.



Figure 4: Correlation Heat Map

3.3.3 Feature Selection Strategies

The features of the proteins and the ligands were selected separately. It helps us make the model plug-and-play as discussed in section 3.1.1. The best combination (Global Optima) cannot be obtained practically by brute force algorithms. This is because one would have to try $\binom{402}{k_1} * \binom{55}{k_2}$ ($k_1, k_2 \in \mathbf{I}^+$) possibilities which is impractical. In the subsequent subsections, a few feature selection strategies considered in this project are discussed.

Selection by output correlation: The *pearson* and *spearman* correlations of each feature were calculated against the output variable. An assumption that the features were either linearly related to the output (in the case of Pearson correlation) or had a monotonic relationship (in the case of Spearman correlation) was made. 20 Ligand descriptors that were the most correlated to the output variable were selected. Similarly, the best 20 protein descriptors that were the most correlated to the output variable were selected.

Using genetic algorithms: Since the feature space is a non-continuous problem of combinatorial complexity, genetic feature selection algorithms [3] were also studied. Each feature was represented by a binary number, 1 for its inclusion and 0 for its exclusion. Let \mathbb{B} be a binary number $\{0, 1\}$. Each feature selection $p \in \mathbb{B}^{456}$ (401 for ligands + 55 for proteins) is called a chromosome (in other words, an individual in a population). A "population"

of n chromosomes is maintained during the algorithm. For each generation, the best chromosomes are selected as parents. The chromosomes of the next generation are generated by doing crossover and mutation of the selected chromosomes. Algorithm 1 below gives complete pseudocode for this.

The scoring function used to select the best chromosome can vary according to the model type. [See Section 4]

Algorithm 1 Selection of features for the model using genetic algorithm [3]

```

1: procedure GENETIC_ALGORITHM_BASED_SELECTOR
2:   scoringfunction  $\leftarrow$  Get model specific scoring function
3:   population =  $\{C_1, C_2, C_3 \dots C_n\} \in \mathbb{B}^{456}$  (initial chromosomes).
4:   best  $\leftarrow C_1$  // Arbitrarily initialized
5:    $i \leftarrow 0$ 
6:    $gen \leftarrow$  number of generations to run.
7:   for  $i < gen$  with step 1 do
8:      $\{S_1, S_2, S_3 \dots S_n\} \leftarrow$  scoringfunction(population)  $\forall S_i \in \mathbf{R}$ .
9:     // Do a tournament selection for the best chromosomes
10:    genetically_better_population  $\leftarrow$  empty list
11:    for  $j < len(population)$  do
12:      Set  $\leftarrow$  random_k_selections(population)
13:       $c \leftarrow best(Set)$  // Based on scoringfunction.
14:      genetically_better_population.add( $c$ )
15:    end for
16:    children  $\leftarrow$  empty list
17:    for  $j < len(population)$  with step 2 do
18:       $P_1, P_2 \leftarrow population[j], population[j + 1]$ 
19:       $c_1, c_2 \leftarrow crossover(P_1, P_2)$ 
20:       $c_1 \leftarrow mutation(c_1)$ 
21:       $c_2 \leftarrow mutation(c_2)$ 
22:      children.add( $c_1, c_2$ )
23:    end for
24:    population  $\leftarrow$  children
25:  end for
26:  return best(population)
27: end procedure

```

Manual Feature selection: A selected list of 121 ligand descriptors was given by Simon Bray. All protein descriptors were used as they were only a

few in number.

3.4 Testing

3.4.1 Reproducibility

Reproducible ML models are very crucial for verifying any project or research results. Due to the stochastic nature of many ML training processes, reproducing the exact model (and consequently the exact output) is a challenge. Two methods can be employed to produce verifiable results:

- Training many models and reporting the average results.
- Controlling the randomness of the trained models. One can set the seed of the pseudorandom algorithms used in the training process to accomplish this.

The second approach is used in this project. Every script, when executed, reports an execution ID. It is the random seed used during the execution. The exact results can be reproduced by using this execution ID as the first argument to the script.

3.4.2 Model Quality Analysis

The following function is predicted by the model

Binding affinity prediction : $\mathbf{R}^n \mapsto \mathbf{R}$ where $n \in \mathbf{I}^+$

Since the input space is multi-dimensional, one cannot fully visualize the model as a function of the input space. To get around this,

- *Coefficient of determination* is reported. $R^2 \in (-\infty, 1.0]$ where 1.0 is the best score. [10]

$$R^2(y, \hat{y}) = 1 - \frac{\sum_{i=1}^n (y_i - \hat{y}_i)^2}{\sum_{i=1}^n (y_i - \bar{y})^2} \text{ where } \bar{y} = \frac{1}{n} \sum_{i=1}^n y_i \text{ and } \sum_{i=1}^n (y_i - \hat{y}_i)^2 = \sum_{i=1}^n \epsilon_i^2$$

- A 2D scatter plot of expected values versus the model's predicted output is plotted.

A perfect model would have all the points on the $y = x$ line. It corresponds to a R^2 score of 1.0. Figure 5, shows the validation accuracy of a sample *Random Forest Regressor* model. $y_validate$ (x axis) represents the actual validation data. $y_validate_pred$ (y axis) represents the predicted output from the model.



Figure 5: (Sample) Visualizing accuracy. $R^2 \approx 0.805$.

4 Results

The following machine learning models were used:

- Linear Regression
- Support Vector Regression
- Rotation Forest Regression
- Random Forest Regression

By far, the most impressive performance was given by Random Forest Regression. Hence more time was spent on the Random Forest regression models to understand the reasons for their good performance.

Because of the lack of data, Deep Neural Networks were not suitable for this project. For example, if all the features were used to train a simple DNN model of size $[457, 20, 10, 1]$, there would be 9350 parameters to train. As only 16,000 data points were present to train the model, the deep learning model would over-fit drastically.



Figure 6: Cumulative PCA of ligand features

4.1 Data Preprocessing

Before fitting the model, a preliminary analysis of the data was performed. This was necessary to train the models more reliably.

4.1.1 Data cleaning

Using principal component analysis (PCA) each feature’s contribution in the variation of the data was analyzed. During this analysis, 2 issues were found:

- There was a ligand feature named IPC which had extremely small and extremely huge values e.g $k * 10^{39}$ where $k \in (0, 1]$. Hence, this feature was scaled using a logarithm function. This was done for numerical safety during the training of the models. Figure 6 illustrates the effect of this scaling on the cumulative PCA.
- There were a lot of NaN (Not a number) and zeros in the data. Perhaps these descriptors did not make sense for some of the ligands. As the presence of 0s was harmless, they were not changed in the input data. However, the NaN values were removed before the data was input into the model. Figure 7 shows cumulative PCA of the protein features.



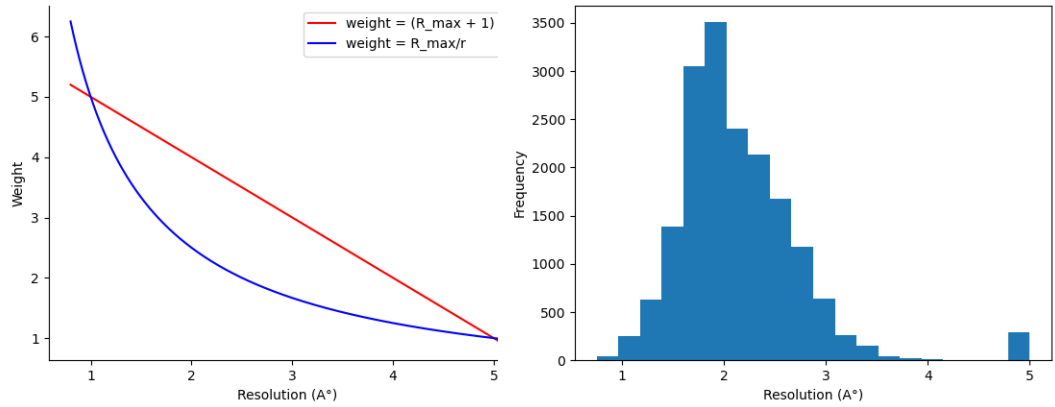
Figure 7: cumulative PCA of protein features

The ligand feature IPC must be scaled before it is input into the model. This is a limitation of the models studied in this project.

4.1.2 Dealing with measurement resolution

Atomic structures produced using X-ray crystallography always have a particular resolution associated with them (\AA units). The structural detail of the 3D image is inversely proportional to the resolution. As shown in a small excerpt of the PDB Databank INDEX file, a resolution measurement for each of the complexes (or data points) is also present in the data.

```
# =====
# List of protein-ligand complexes with known binding data in PDBbind v.2019
# 17679 protein-ligand complexes in total, sorted by binding data
# Latest update: Dec 2019
# PDB code, resolution, release year, -log Kd/Ki, Kd/Ki, reference, ligand name
# =====
3zzf  2.20  2012  0.40  Ki=400mM      // 3zzf.pdf (NLG)
3gww  2.46  2009  0.45  IC50=355mM    // 3gww.pdf (SFX)
```

(a) Weight calculation formulae

(b) Resolution distribution

Figure 8: Weight calculation and resolution distribution

1w8l 1.80 2004 0.49 Ki=320mM // 1w8l.pdf (1P3)

Using the resolution, the following 2 ways to calculate the weight of each data point were devised.

- Hyperbolic formula: $W_i = \frac{\max R_{1\dots n}}{R_i}$
- Linear formula: $W_i = (\max R_{1\dots n} + 1) - R_i$

Here, R_i is a resolution of a given data point. It was found that $\max R_{1\dots n} \approx 5 \text{ Å}$ in the data. 1 was added to the max resolution in the linear formula to avoid data points with 0 weight. Figure 8a depicts the formulae. Figure 8b shows the distribution of data points as a function of resolution. The resolution of the measurements ranges from 1 Å to 5 Å approximately.

Figure 9 shows the distribution of the weights obtained from the data for the linear and hyperbolic case. Figure 9b shows that linear weighting of data points results in data points with a higher weight as compared to hyperbolic weighting. This makes intuitive sense. As shown in Figure 8b, most of the data points have a resolution around 2 Å. Since linear weighting around 2 Å is higher, the linearly weighted data points will have a higher weight on average.

The calculated weights were used in two ways during the model training

- Duplicating the data points.

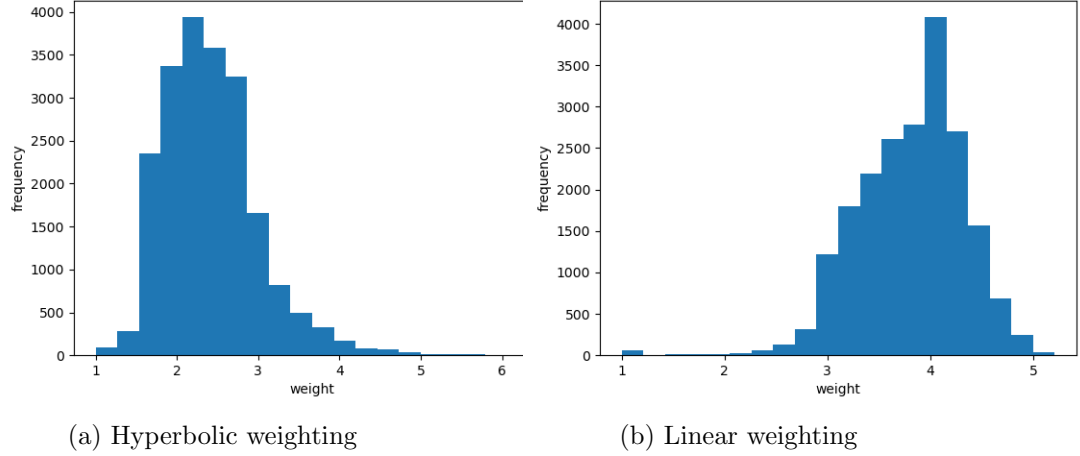


Figure 9: Weighting of the data points (Excluding the test set)

- Using the weights directly in the fit function.

After the duplication, ≈ 39000 data points were obtained for the linear weighting formula and ≈ 62000 for the hyperbolic weighting.

4.2 Linear regression

Linear regression fits a linear model to a given data. It tries to minimize the square of errors between the predicted output value and the actual output value. It was the cheapest model (computationally) that was used to fit the data. Table 1 shows the overview of the analysis with this model. Figure 10 shows the best results obtained with linear regression.

| No. features | Feature selection | Weighting | Training | Validation | Testing |
|--------------|----------------------|------------------------|-----------------|-----------------|-----------------|
| 457 | - | - | 0.456 | 0.433 | 0.412 |
| 457 | - | Hyperbolic | 0.452 | 0.431 | 0.420 |
| 457 | - | Hyperbolic duplication | 0.465 | 0.424 | 0.419 |
| 457 | - | Linear | 0.455 | 0.430 | 0.416 |
| 457 | - | Linear Duplication | 0.460 | 0.428 | 0.407 |
| 49 | Genetic ¹ | Hyperbolic | ≈ 0.373 | ≈ 0.393 | ≈ 0.402 |
| 40 | Pearson Correlation | Hyperbolic | 0.288 | 0.276 | 0.286 |
| 40 | Spearman Correlation | Hyperbolic | 0.291 | 0.280 | 0.289 |
| 176 | Manual | Hyperbolic | 0.364 | 0.342 | 0.389 |

Table 1: R^2 scores of the Linear Regression Model

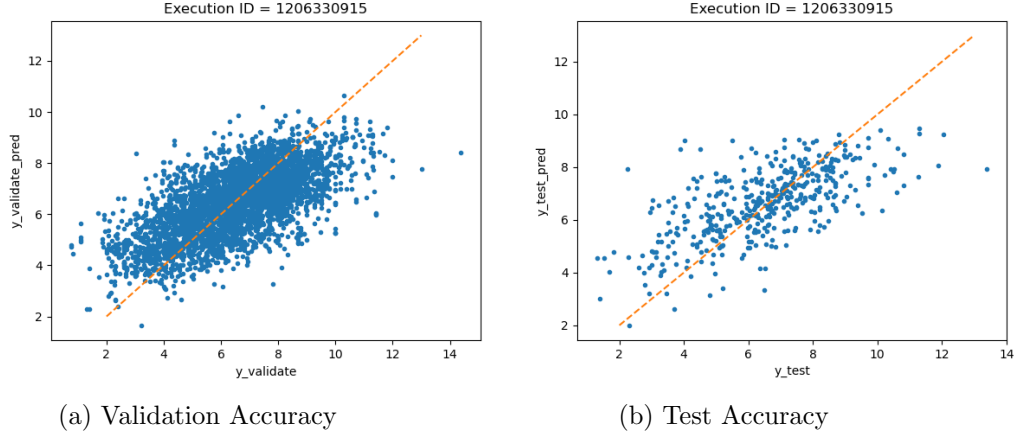


Figure 10: Linear Model using Hyperbolic weighting and all 457 features.

The reason for the low R^2 score is that linear models assume strong linearity between the input variables and the output variable. This is not always true. One anomaly in the results is that there are some cases where the validation and testing results seem to be better than the training result. However, this is not always the case. The results highly depend on the seed. If the seed changes, the train/test data split gives different data for training and validation. What is important for the validity of the model is that the results remain in a reasonable range.

In the linear regression model, genetic algorithms were used to reduce both the large feature space and to eliminate the correlated features within families.

4.2.1 Score function of genetic feature selection

Because the linear regression model was computationally cheap, refitting the model multiple times in the genetic algorithm was affordable. There were two objectives at hand

- Getting the best performing model.
- Reducing the number of input features to make the model simple and explainable.

¹Approximately reproducible as the reproducibility module was introduced later.

The above objectives were not always against each other. This is because removing a feature that has no correlation (or random correlation) with the output may improve the model. On the other hand, removing a feature that is ‘correlated with the output degrades the model.

Hence, taking inspiration from the hypervolume-based multi-objective optimization, the following score function was designed.

$$\text{score} = \mathbf{R}^2\text{score} * \text{Features Eliminated}$$

Figure 11 provides a graphical depiction of the score function. Here the score function represents the area of the square formed between a given point and the origin. Trying to improve the score means, it will try to eliminate more features as well as try to get a higher R^2 score. In the example below, the point a is preferred over b as it gives almost the same R^2 score and eliminates a larger number of features. Another advantage of this score function is that one does not need to keep the values of both components (i.e. *features eliminated* and R^2 score) in a similar range. Hence one need not worry about scaling any of these components.

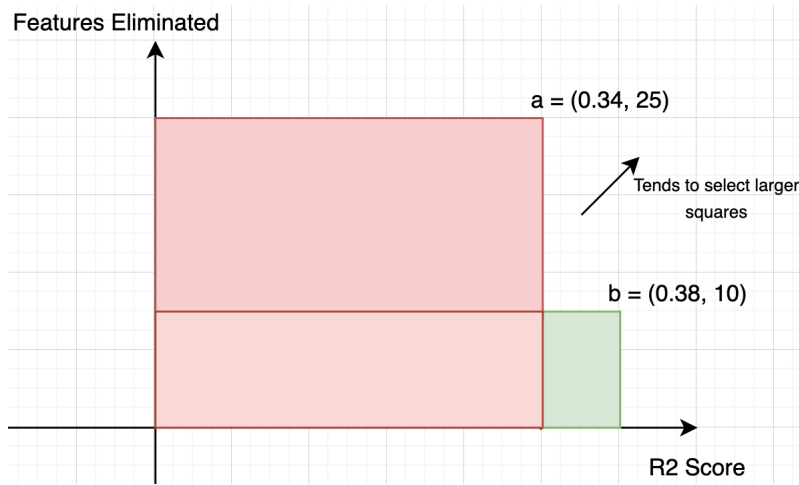


Figure 11: Genetic Algorithm score function representation.

4.2.2 Initialization strategies of population

Two main strategies were used to initialize the population for the genetic algorithm:

- **Random Initialization.** A population of 2400 chromosomes was randomly initialized and run for 500 generations.
- **Specific Initialization.** Here, the initial population was kept at 457. The algorithm was run for 2000 generations. Each chromosome in the population had 1 distinct feature excluded. The following represents the initialization of the chromosomes.

$c_1 = [01111.....11]$
 $c_2 = [10111.....11]$
 $c_3 = [11011.....11]$
...
 $c_{457} = [11111.....10]$

The rationale was that using the above score function, a local minimum could be obtained by eliminating the worst performing features rather than trying to select the best performing features as in the case of random initialization.

Both the initialization strategies gave similar results as shown in Table 1.

4.3 Random Forest Regression

Random forest regression is an ensemble ML model of regression trees. When training each tree, the algorithm finds out which feature value can divide the data into 2 groups to yield the lowest sum of squared values on both sides (The criterion can be different as well e.g. lowest absolute error). Then each of the sub-data is split recursively till a stopping criterion (e.g. a set number of data points in the leaf).

For each tree, a subset of the data is used for training. The subset of data is sampled with replacement a.k.a bagging. After training, the bunch of "Experts" that are good at different data subsets predict the output of new given inputs. The average of the predicted outputs is the result of the whole random forest regressor.

This model is non-linear. One advantage is that there is no need for any assumption about the data. Moreover, random forests can handle categorical features together with the real-valued features very easily. On the negative side, the function represented by the ensemble cannot be easily represented and has to be interpreted as a black-box function.

Figure 12 shows the validation and testing accuracy obtained by a random forest with manually selected features. This model outperforms the other features selection strategies.

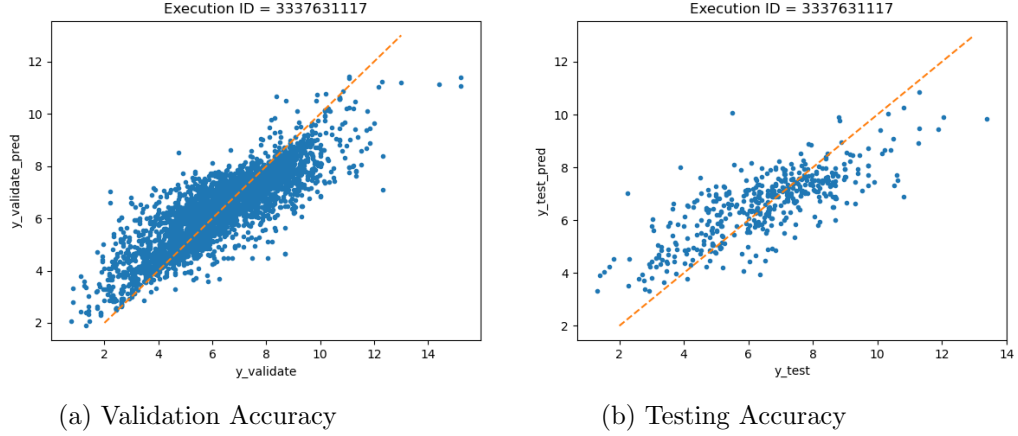


Figure 12: Random Forest Regressor with 176 manually selected features and hyperbolic weighting.

Table 2 gives an overview of our model. The table shows that features selected by output correlation (Spearman and Pearson correlations) seem to generalize well to the test data. However, one cannot consider this as a good model because the validation error and the test error are not in agreement with each other. Moreover, the correlated feature selection assumes that the data features have a strong linear or monotonic relation with the output which may not be correct in our case. Hence, these models were not considered to be the best models.

| No. Features | Feature Selection | Weighting | Training | Validation | OOB score | Testing |
|--------------|----------------------|-------------------|--------------|--------------|--------------|--------------|
| 457 | - | - | 0.961 | 0.790 | 0.793 | 0.540 |
| 457 | - | Hyperbolic | 0.961 | 0.778 | 0.796 | 0.555 |
| 457 | - | Linear | 0.960 | 0.800 | 0.790 | 0.542 |
| 40 | Spearman Correlation | Hyperbolic | 0.930 | 0.677 | 0.672 | 0.880 |
| 40 | Pearson Correlation | Hyperbolic | 0.925 | 0.651 | 0.646 | 0.870 |
| 229 | Genetic Elitism | Hyperbolic | 0.958 | 0.791 | 0.792 | 0.537 |
| 394 | Genetic Normal | Hyperbolic | 0.960 | 0.808 | 0.791 | 0.543 |
| 176 | manual | Hyperbolic | 0.947 | 0.737 | 0.734 | 0.579 |

Table 2: Random Forest Regression R^2 Score table

4.3.1 Dealing with correlated features

In Section 3.3.2 it was discussed that within some of the families of features there are heavily correlated features. One way to deal with this would be

to just take one feature from a family and exclude the rest. However, this would not be a good strategy for generalization. This is because our trained model would be unusable by someone who could not measure one of these selected features (or if the measurements were incorrect).

For this reason, the stochasticity of the random forest was used as an advantage. During the creation of a regression tree, the random forest model tries to get the best (feature, value) tuple to divide the data. This is known as the split criterion. The model was forced to randomly select only 20% of the features for deciding on the split criterion. More specifically, the following values were used

- 400 Trees (n_estimators)
- 20% of feature selection (max_features). This increased the stochasticity of the model.
- A minimum of 2 data points for each leaf. (min_samples_leaf)

These hyperparameters were determined after some empirical testing. The number of estimators had to be increased as the stochasticity of our ensemble was higher. Our model would hence be dependent on the entire family of features and not rely on a single feature heavily.

4.3.2 Dealing with measurement resolution

The model was trained by duplicating the data according to their weights. The following results were obtained after training - Training R^2 score = 0.995, Validation R^2 score = 0.8298 and Out Of Bag (OOB) score = 0.977.

The following issues were found with this strategy:

- The out-of-bag error (OOB score) is erroneously high here. This is because of repeated data points. Many points are both inside the selected bag and outside it.
- Due to duplication of data points, the trees may end up being more correlated to each other. This will affect the generalization of our model.
- As training this model is costly, duplicating the data points further increases the cost of training.

Hence, it was concluded that the duplication of data based on their weights is a wrong strategy for this model.

When the weights were directly used in the fit function, no noticeable improvement was seen in our model. This is because the data is already skewed towards the ≈ 2 Å data points. This can be seen in Figure 8b.

4.3.3 Feature Importance calculation

The Random Forest regression model fitting is very expensive as compared to the simple linear regression. For example in a machine with 4 CPUs, fitting a linear model on our data takes ≈ 0.51 seconds whereas fitting the random forest model takes ≈ 25.86 seconds. Hence the same strategy cannot be used for feature selection as used in the linear models. The following strategies were used to determine the importance of features in the model.

- **Gini Importance (or) Decrease in impurity.** This is calculated by the model itself. For every feature, it calculates how much decrease in the split criterion the feature contributes in the entire ensemble (i.e in every node it's used in all the trees). The disadvantage is that they cannot be reliable when the features have a high cardinality. Figure 13a illustrates this importance.
- **Permutation Importance** - This is a model agnostic method. To calculate the importance of a feature x , it takes the given data and shuffles the values of x . Now the values of feature x do not correspond to the correct data points, hence there is a reduction in the prediction accuracy. The importance of the feature is proportional to the reduction in accuracy. The disadvantage of this method is that since each feature is checked independently, correlated input features make the results unreliable. If feature A and feature B are correlated, the shuffling of A may not impact the model as the model can rely on B for its prediction. Figure 13b illustrates this importance.

4.3.4 Permutation Importance and genetic algorithm

To overcome the issue with the above feature importance selection, a combination of permutation importance and genetic algorithms was used to find out the importance of the selected features. This is because it was expensive to refit the model. However, it was cheap to evaluate the predicted results of the model after shuffling the features.

The following 2 strategies were used with the genetic algorithms -



Figure 13: Feature Importance calculation of Random Forest Regressor. (With manual feature selection)

- **Using specific scoring function.** In Section 4.2.1, the intuition behind the scoring function was discussed. In the random forest model, however, this scoring function selected a lot of features (> 400). Hence the following scoring function was used to reduce the number of features.

$$\text{score} = \mathbf{R}^2 * \text{Features Eliminated}^2$$

A stronger signal was used for the number of eliminated features. This scoring function, however, turned out to be too strong and none of the features were selected.

- **Elitism.** Elitism is a strategy used in the genetic algorithms to select the top few elements from each generation for the next generation in addition to the newly created children. This keeps the best performing subset of the population always in the current generation to improve them further by cross-over or mutation.

4.4 Support Vector Regression

Support vector regression is a non-linear regression method that fits a curve such that the margin of error between the model's prediction and the original value is kept within a minimum range. Any error higher than this minimum range is penalized during the training of the model. Support vector regression was trained with the RBF kernel.

| No. Features | Feature Selection | Weighting | Training | Validation | Testing |
|--------------|----------------------|---------------|--------------|--------------|--------------|
| 457 | - | - | 0.310 | 0.308 | 0.356 |
| 457 | - | Hyperbolic | 0.325 | 0.326 | 0.371 |
| 457 | - | Linear | 0.336 | 0.334 | 0.374 |
| 40 | Spearman Correlation | Linear | 0.256 | 0.286 | 0.262 |
| 40 | Pearson Correlation | Linear | 0.199 | 0.200 | 0.199 |
| 40 | Spearman Correlation | Hyperbolic | 0.252 | 0.266 | 0.254 |
| 40 | Pearson Correlation | Hyperbolic | 0.169 | 0.169 | 0.169 |
| 176 | Manual | Linear | 0.306 | 0.298 | 0.358 |

Table 3: Table showing R^2 Scores for SVR

Data duplication strategy was not used for this model because the training time complexity is $O(n^2)$ where n is the number of data points. However, the data point weights were used during the fit function of the training.

The results are reported in Table 3. The linear weighting of the data gave the best results in SVR. The reason testing R^2 score is around the same range as the training score maybe because the testing data is of better quality data as compared to the validation data. However, this varies very highly depending on the random seed used. What must be observed is that the approximate range in which the values are obtained is small.

As the performance of the model was not on par with other models, the costly genetic algorithm for feature selection was not run on SVR. Moreover, the time it took to get the R^2 score (validation and testing) was very high and was not suitable to be used in a permutation-based genetic algorithm as discussed in the random forest section. The issues of within family feature correlation as well as feature selection were hence dealt with by either using output correlation or by manual feature selection.

Figures 14a and 14b visualize the validation and testing accuracy of the best SVR model.

4.5 Rotation Forests

In Section 4.3 different strategies to improve the performance of the model were analyzed. While fitting a tree, the random forest model tries to get a (feature, value) tuple that best divides our data. The criterion is to reduce the entropy of the divided data. This is done recursively till some set criteria (E.g., the leaf nodes should contain 7 data points). However, each (feature, value) only represents an axis-aligned hyperplane.

If there are some real-valued features in our data set, one could reduce the complexity of our tree by using a hyperplane that is not axis aligned.

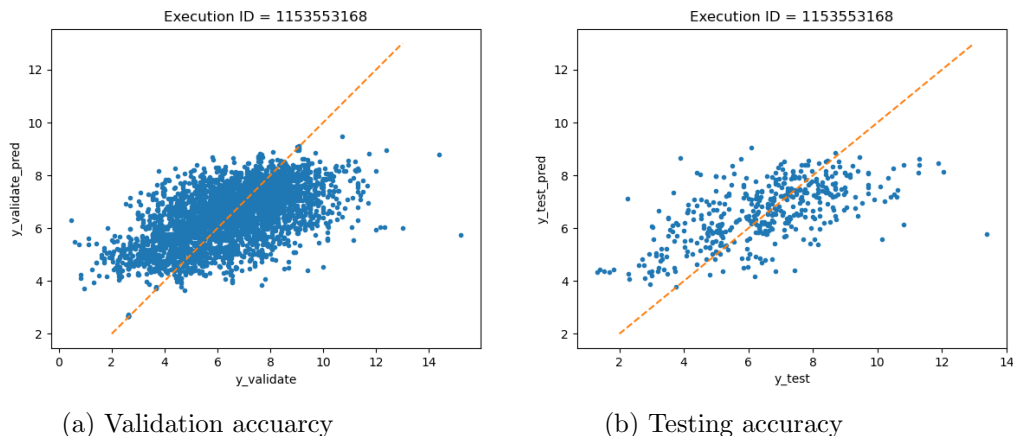


Figure 14: SVR accuracy visualization for all features 457 and Linear weighting

For example consider approximation of the line $y = x$. To approximate this using an axis-aligned hyperplane, one would require a deep tree of high complexity. If instead, the data can be transformed such that the line $y = x$ transforms to $y = k$ where $k \in \mathbf{R}$, only require 1 (feature, value) tuple is required.

This can be accomplished by calculating the eigenvector of our data and transforming our feature space such that the basis vectors are the eigenvectors of the data. Rotation forests use this concept to reduce the complexity of their trees and to get a better quality model. They were first proposed for classification. The implementation for the regression case was adapted in this project.

The training R^2 score was comparable to that of the random forest regressor. However, a considerable improvement in the accuracy was not seen. One of the reasons, is that rotation forests are shown to be better than random forests only for the continuous feature values. However, the data set has both real-valued and discrete values (although the discrete values are encoded as real-values for our model). Hence it was concluded that this model is not the best model for the Protein-Ligand binding affinity prediction.

Table 4 gives an overview of the performance of Rotation forests. The implemented model does not have an option to train weighted data. The models trained by using features selected by output correlation were not considered good models for similar reasons as discussed in Section 4.3.

| Features Selected | Training | Validation | Testing |
|------------------------|--------------|--------------|--------------|
| 457 (all) | 0.967 | 0.756 | 0.543 |
| 457 (Hyperbolic) | NA | NA | NA |
| 457 (Linear weighting) | NA | NA | NA |
| 40 (Person) | 0.948 | 0.596 | 0.878 |
| 40 (Spearman) | 0.951 | 0.667 | 0.896 |
| 176 (manual) | 0.960 | 0.724 | 0.572 |

Table 4: Rotation Forest R^2 Score overview

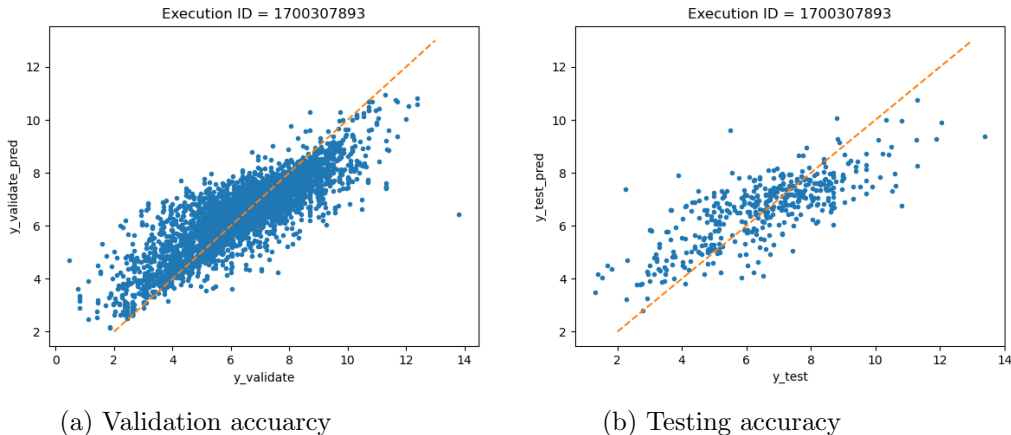


Figure 15: Rotation Forest Accuracy visualization for manually selected features (176). The rotation forest implementation does not support data weighting.

Figures 15a and 15b visualize the validation and testing accuracy of the best Rotation Forest Model.

5 Discussion

In this project, the protein-ligand binding affinity was determined using spatial features extracted by RDKit and D-Pocket. The 2D/3D features made the data more accessible to simple machine learning models. It was crucial because the complex models that directly get the 3D features from the data (E.g., 3D convolutions) require expensive to accumulate data.

Most of the time was spent on analyzing and studying the most suitable

linear model (Linear Regression) and non-linear model (Random Forest Regression) for our extracted data. Our study also included feature selection methods like genetic algorithms. It was found that the extracted protein-ligand data had the following interesting properties

- The data does not have a symmetric Gaussian distribution. In other words, the ranges of values in each dimension were very different.
- The features are both real-valued numbers as well as discrete. The discrete values are also represented as real numbers.
- There are feature families in the ligand descriptors that have highly correlated features.

While Linear Regression did give reasonable results, it was not a very reliable model because it assumed that the data was linearly related to the binding affinity. Nevertheless, genetic algorithms were run on this model to get the best ≈ 50 features. This could not be accomplished in the case of Random Forest Regression models.

Our study found that genetic algorithms were not very helpful in improving the performance of our model. However, they were successful in eliminating around 200 features for the Random Regression Model and around 400 features in the Linear Regression model without hampering the performance to a large degree.

One issue with feature selection algorithms is that they make the model depend on the selected features. This would hamper the model generalization. A single unavailable feature or a single feature measured incorrectly would render our model useless. This hard constraint may not be good when the data collection process is expensive and error-prone.

The Random Forest Regression model could deal with all the above specific properties of our data. Random Forest Regression deals with both Real valued and discrete input features because the main aim of a fitting tree (in the random forest) is to reduce the entropy of the divided data. Since all the discrete features in our data were extracted as real-valued numbers, the trees can easily find a midpoint between the discrete values to divide the data. Interestingly, the feature correlation within families can be used as an advantage to improve the robustness of the model. By increasing the randomness of our feature selection during the data split the model is forced to rely less on a specific feature. Hence a wrong measurement or a corrupted feature would not hamper our model significantly.

Since the random forest model gives an R^2 score of > 0.5 consistently, the binding affinity predicted by the model for any new PL complex can be

taken as a reference for the drug-testing decisions. For example, one can use the results to prioritize testing of new ligands in a wet lab experiment to save resources for the important ligands.

As with any model, the model and approach do have limitations. Firstly, Random Forest Regression models cannot be explained easily. With hundreds of trees in our random forest, the model at best can only be treated as a Black Box. Because of its complexity, we were not able to show why some features were very important as compared to the others (E.g., in the feature importance calculation). Secondly, our model relies heavily on the ligand features. The model, hence, assumes that the binding only slightly depends on the protein features. On the contrary, the protein and ligand features are both equally responsible for the binding affinity. Also, hyper-parameter optimization could not be performed in conjunction with the genetic feature selection algorithms as it was prohibitively expensive.

6 Conclusion

In this project, we studied methods and preprocessing techniques to predict the protein-ligand binding affinity. In conclusion, we suggest using Random Forest Regression for this problem because of the ease of training and the generalization capability. We believe that a random forest regression could be used as a baseline to compare any new models.

In further work, we believe that there is scope for improving the feature selection process of our model. Our model depends heavily on the ligand features as compared to the protein features. We believe it is because of the data extracted by RDKit and D-Pocket. Further investigation on new models that do not have this limitation would be helpful. One way could be to build models with all protein features and one family of ligand features. The most important features in each family may can as surrogates for the whole family. We also think more study needs to be conducted to create explainable models. It would be both accepted by the Cheminformatics community and would be helpful to further the understanding of binding affinity.

References

- [1] Protein Data Bank. Example Protein - 2Y07. [Link](#). [Online; accessed 1-Aug-2021].

- [2] Uni-Freiburg) Björn Grüning (Department of Bioinformatics. Galaxy Tool wrappers. [Link](#). [Online; accessed 1-Aug-2021].
- [3] Jason Brownlee. Simple Genetic Algorithm From scratch. [Link](#). [Online; accessed 28-June-2021].
- [4] TMP Chem. Computational Chemistry 1.2 - PDB File Format. [Link](#). [Online; accessed 22-July-2021].
- [5] Vincent Le Guilloux and Peter Schmidtke. fpocket User Manual. [Link](#). [Online; accessed 2-Aug-2021].
- [6] Abdus Salam Khazi. Code for the whole project. [Link](#). [Online; accessed 22-July-2021].
- [7] PDBank. PDBank History. [Link](#). [Online; accessed 22-July-2021].
- [8] PDBank. PDBank Homepage. [Link](#). [Online; accessed 22-July-2021].
- [9] RDKit. RDKit: Open-Source Cheminformatics Software. [Link](#). [Online; accessed 1-Aug-2021].
- [10] scikit learn. R2 score, the coefficient of determination. [Link](#). [Online; accessed 22-July-2021].
- [11] The Science Snail. Difference between Ki, Kd, IC50 and EC50 values. [Link](#). [Online; accessed 22-July-2021].
- [12] Wikipedia. Docking (molecular). [Link](#). [Online; accessed 1-Aug-2021].
- [13] Wikipedia. PDBbind database. [Link](#). [Online; accessed 22-July-2021].
- [14] Wikipedia. Protein Data Bank (file format). [Link](#). [Online; accessed 22-July-2021].
- [15] Wikipedia. Protein–ligand complex. [Link](#). [Online; accessed 24-June-2021].
- [16] Wikipedia. Simplified molecular-input line-entry system. [Link](#). [Online; accessed 1-Aug-2021].
- [17] Wikipedia. Structure Data File format. [Link](#). [Online; accessed 1-Aug-2021].
- [18] Wikipedia. XYZ Format. [Link](#). [Online; accessed 22-July-2021].
- [19] Gaming World. Procedural Terrain Generation with Unity : What is Voronoi Tessellation. [Link](#). [Online; accessed 2-Aug-2021].

7 Appendix

7.1 XYZ File format

The following represents the pyridine molecule in the XYZ format.

11

| | | | |
|---|--------------|--------------|--------------|
| C | -0.180226841 | 0.360945118 | -1.120304970 |
| C | -0.180226841 | 1.559292118 | -0.407860970 |
| C | -0.180226841 | 1.503191118 | 0.986935030 |
| N | -0.180226841 | 0.360945118 | 1.29018350 |
| C | -0.180226841 | -0.781300882 | 0.986935030 |
| C | -0.180226841 | -0.837401882 | -0.407860970 |
| H | -0.180226841 | 0.360945118 | -2.206546970 |
| H | -0.180226841 | 2.517950118 | -0.917077970 |
| H | -0.180226841 | 2.421289118 | 1.572099030 |
| H | -0.180226841 | -1.699398882 | 1.572099030 |
| H | -0.180226841 | -1.796059882 | -0.917077970 |

7.2 SDF File format

2uzn_ligand

```
Created by X-T00L on Fri Nov 18 14:55:27 2016
37 39 0 0 0 0 0 0 0 0999 V2000
    7.1480    60.4530    6.6830  0 0 0 0 1 0 1
    6.0470    60.1670    7.5640  S 0 0 0 1 0 4
    .....
    .....
   -2.6338    67.4589    8.1225  H 0 0 0 1 0 1
  1  2  2  0  0  2
  2  3  2  0  0  2
    .....
    .....
23 37  1  0  0  2
M  END
> <MOLECULAR_FORMULA>
C15H13N3O4S2

> <MOLECULAR_WEIGHT>
```


363.3

> <NUM_HB_ATOMS>

7

> <NUM_ROTOR>

1

> <XLOGP2>

1.31

7.3 MOL2 File Format

###

Created by X-T00L on Fri Sep 26 17:34:18 2014

###

@<TRIPOS>MOLECULE

1fo2_ligand

25 25 1 0 0

SMALL

GAST_HUCK

@<TRIPOS>ATOM

| | | | | | | | | |
|---|----|---------|---------|---------|-----|---|-----|--------|
| 1 | C4 | 39.0090 | 40.2680 | 25.5130 | C.3 | 1 | DMJ | 0.1280 |
|---|----|---------|---------|---------|-----|---|-----|--------|

| | | | | | | | | |
|---|----|---------|---------|---------|-----|---|-----|---------|
| 2 | O4 | 39.2170 | 40.5810 | 26.8980 | O.3 | 1 | DMJ | -0.3835 |
|---|----|---------|---------|---------|-----|---|-----|---------|

.....

| | | | | | | | | |
|----|-----|---------|---------|---------|---|---|-----|--------|
| 25 | H14 | 38.0787 | 41.8134 | 21.3802 | H | 1 | DMJ | 0.2097 |
|----|-----|---------|---------|---------|---|---|-----|--------|

@<TRIPOS>BOND

| | | | |
|---|---|---|---|
| 1 | 1 | 9 | 1 |
|---|---|---|---|

| | | | |
|---|---|---|---|
| 2 | 1 | 3 | 1 |
|---|---|---|---|

.....

| | | | |
|----|----|----|---|
| 25 | 11 | 25 | 1 |
|----|----|----|---|

@<TRIPOS>SUBSTRUCTURE

| | | |
|---|-----|---|
| 1 | DMJ | 1 |
|---|-----|---|

7.4 Correlation Heat Maps

This section shows the correlation heat maps of the most interesting feature families in the our dataset.



(a) Family EState_VSA



(b) Family PEOE_VSA



(c) Family SMR_VSA



(d) Family fr_



(e) Family SlogP_VSA



(f) Family VSA_EState

Figure 16: Correlation Heat Maps